

Resonant enhancement of rare-earth valence-band photoemission at 3*d* absorption edges.

J. W. Allen and S.-J. Oh

Xerox Palo Alto Research Center, 3333 Coyote Hill Road, Palo Alto, California 94304

I. Lindau

Stanford Synchrotron Radiation Laboratory, Stanford, California 94305

L. I. Johansson

Linköping University, S-581 83 Linköping, Sweden

(Received 26 September 1983)

We report the first observation of resonant enhancement of rare-earth 4*f* photoemission for photon energies at the rare-earth 3*d* absorption edge. The 3*d* edge resonance is intrinsically weaker than that at the 4*d* edge, but has a larger on- to off-resonance ratio. This and other properties of the 3*d* resonance open up new possibilities for spectroscopic applications.

The large resonant enhancement of rare-earth valence-band photoemission for photon energies near the 4*d* absorption edge is a phenomenon that has been intensely studied and developed as a spectroscopic technique by many workers since it was first observed¹⁻³ five years ago. The resonance can be thought of as the photon absorption process $4d^{10}4f^n \rightarrow 4d^94f^{n+1}$ followed by the Auger decay $4d^94f^{n+1} \rightarrow 4d^{10}4f^{n-1} + \text{photoelectron}$. It has been speculated both privately and in the literature⁴ that similar effects would occur at the absorption edges of deeper core levels, such as the 3*d* edges, and a 3*d* resonance of 4*f* inverse photoemission has been reported.⁵ Here we report the first observation of such resonant enhancement of valence-band photoemission for the photon energy near the 3*d* absorption edge, and for comparison, 4*d* resonance data on the same samples. The ratio of on-resonance to off-resonance intensity is very much greater for the 3*d* resonance than for the 4*d* resonance, although we give an analysis showing that the 3*d* resonance is intrinsically weaker, as might be expected since the 3*d* resonance is of Koster-Kronig type while the 4*d* resonance is of the super-Koster-Kronig type.⁶ We set forth below some exciting advantages of the 3*d* resonance over the 4*d* resonance for spectroscopic applications, especially to cerium and other mixed-valent rare-earth materials. These results suggest the merits of including improved photon fluxes in this energy range, 800–1600 eV, in existing synchrotron radiation facilities and in the planning for future beam lines.

The experiment was performed at the Stanford Synchrotron Radiation Laboratory. Polycrystalline samples of TbCo₂ and CeAl having 5×5 mm² cross sections were fractured and measured under a vacuum of 1×10⁻¹⁰ Torr in a vacuum chamber equipped with a commercial cylindrical mirror electron-energy analyzer (CMA). Photons with energies near the rare-earth 4*d* edges were obtained using the grasshopper monochromator⁷ on beam I-1, and the combined monochromator-CMA resolution was 0.8 eV. Photons with energies near the rare-earth 3*d* edges were obtained using beryl crystals in the double-crystal (JUMBO) monochromator⁸ on beam line III-3, which yields a photon resolution of 0.5 eV at 890 eV and 0.7 eV at 1250 eV, the Ce and Tb 3*d* core-level regions, respectively. The beam size from this monochromator is 2×4 mm². Calibration

was performed at the Cu 2*p*_{3/2} edge energy, taken as 931.1 eV, and the energy uncertainty may be as large as 1 eV at the Tb 3*d* edges where crystal angle is much larger. The JUMBO throughput is maximum at the Tb 3*d* edge and nearly minimum at the Ce 3*d* edge, so that the signal-to-noise ratio of the data obtained for CeAl is adequate only to show that the resonance occurs. The photon flux available dictated operating the CMA so that the total monochromator-CMA resolution was 3.25 eV for the CeAl photoemission spectra and 1.75 eV for the TbCo₂ spectra. The actual count rates obtained for all the photoemission data reported here are stated in the captions for Figs. 1, 3, and 5.

Figure 1 shows the valence-band photoemission of TbCo₂ for photon energies below and at the Tb 4*d* edge. The Tb 4*f*⁸ → 4*f*⁷ spectral weight is the small peak labeled B, which is the 4*f*⁷ (⁸S_{7/2}) ground state, and the large peaks centered around 10 eV, which are excited multiplets of 4*f*⁷. The emission beginning at the Fermi level *E*_F, is from hybridized Co and Tb conduction band states. The Tb 4*f* emission is a broadened version of that observed⁹ in Tb metal and the broadening is intrinsic, not instrumental, as tested by taking spectra with higher CMA resolution. Such broadening is known in some cases to be inhomogeneous, associated with surface shifts, although we have not investigated this possibility for TbCo₂. The Co 3*d* states tend to dominate the 120-eV spectrum, while the two spectra at the 4*d* edge show great enhancement of Tb 4*f* and 5*d* states. For the 4*f* emission at 10 eV, the ratio of intensity in the on-resonance 156-eV spectrum to that of the off-resonance 120-eV spectrum is ~5. Figure 2 shows, in the energy range of the 4*d* edge, the photon-energy dependence of emission intensity at two points of the valence-band spectrum [constant-initial-state (CIS) spectra] and of the emission intensity at a low kinetic energy fixed in the inelastic tail [constant-final-state (CFS) spectrum], which is generally taken to be proportional to the absorption constant.⁴ These spectra show a rich structure due to multiplets of the 4*d*⁹4*f*⁹ configuration, and as commonly occurs, different intermediate states resonate different parts of the photoemission spectrum with differing intensities. It is apparent that a photon energy of 120 eV is sufficiently below the rather broad resonance region to yield a spectrum typical of being off resonance.

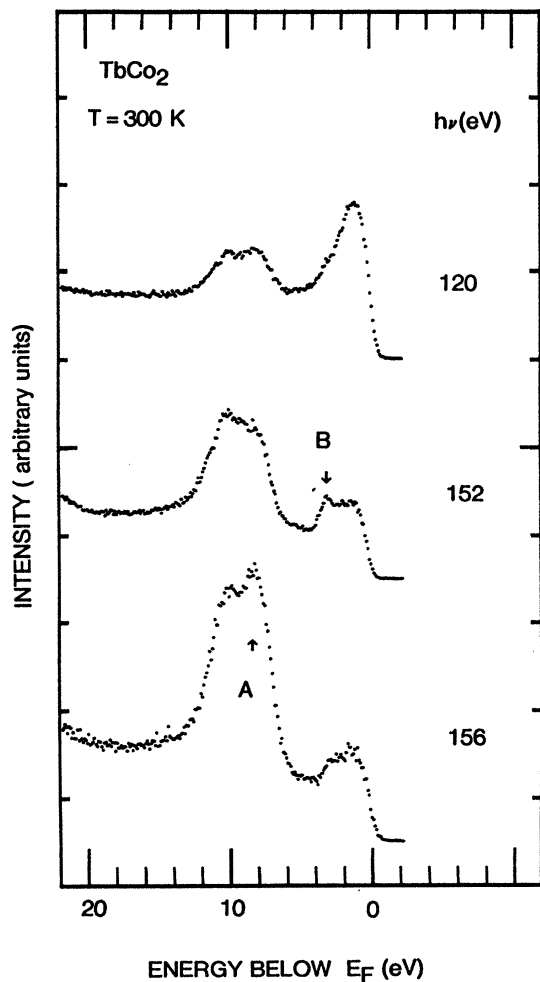


FIG. 1. Valence-band emission of TbCo_2 for several photon energies below and at the Tb $4d$ absorption edge. The labels A and B mark the initial states of the CIS spectra shown in Fig. 2. Curves have vertical zeros, defined by their portions above E_F , displaced upward from the figure boundary by 0.5, 3.5, and 6 units, but all have the same vertical scale, for which one unit is 2000 counts/sec.

The basic aspects of the $3d$ resonance appear in Fig. 3, which shows the valence-band photoemission of TbCo_2 for photon energies below and at the Tb $3d$ edge, and in Fig. 4, which shows CFS and CIS spectra for this photon-energy range. Comparing Figs. 1 and 3 shows the differing resolutions mentioned above, and comparing Figs. 2 and 4 shows that for the $3d$ edge the structure of the CIS and CFS spectra is dominated by the Tb $3d$ spin-orbit splitting, while multiplets of $3d^9 4f^9$ are a small perturbation. It is apparent that a photon energy of 1229 eV yields an off-resonance spectrum. Two other aspects of the data stand out. First, for the $4f$ emission at 10 eV, the ratio of intensity in the on-resonance 1236-eV spectrum to that in the off-resonance 1229-eV spectrum is 72, considerably larger than the equivalent value of 5 for the $4d$ resonance. Second, the higher energy set of intermediate states is much less efficient in the resonance than is the lower-energy set, especially for valence-band states near E_F . These valence-band

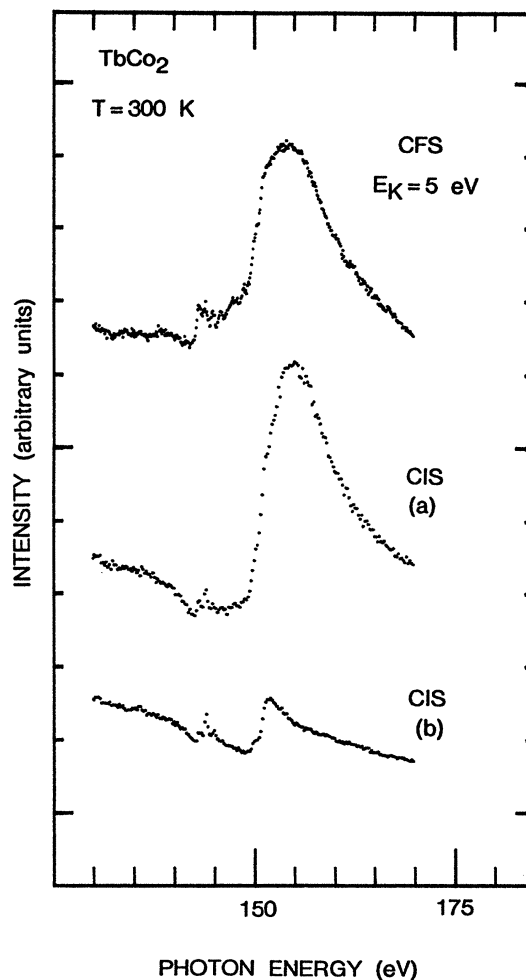


FIG. 2. CFS and CIS spectra for TbCo_2 for photon energies in the $4d$ absorption region. The CIS spectra (a) and (b) are taken for the initial states labeled A and B, respectively, in Fig. 1.

states are either the 8S part of the $4f$ emission, or the Tb $5d$ emission, which tend to be mixed for the experimental resolution. It is not obvious what effect or selection rule is operating to produce this result, but it may be useful spectroscopically, as described below. For the Tb $4d$, $5s$, and $5p$ levels, we have also observed resonant photoemission for this photon-energy range, but the spectra are too greatly complicated by Auger emission to describe in detail here. Figure 4 shows a CIS spectrum for the $4d$ region.

Figure 5 shows CFS and CIS spectra for CeAl for the photon-energy range around the Ce $3d$ edge. For this material it is known¹⁰ that all the cerium $4f$ and $5d$ emission occurs in the first 2 eV below E_F , and since the low-photon intensity limited the experimental resolution to 3.25 eV, no detailed features of the valence band could be resolved. In contrast to the $4d$ CIS spectrum, the CIS spectrum for the broadened valence band is seen to resonate at the lower-energy $3d$ absorption, but hardly at all at the upper-energy absorption, similar to the finding for Tb. The photon flux was too low to obtain a valence-band spectrum off-resonance, and so a value of the on- to off-resonance in-

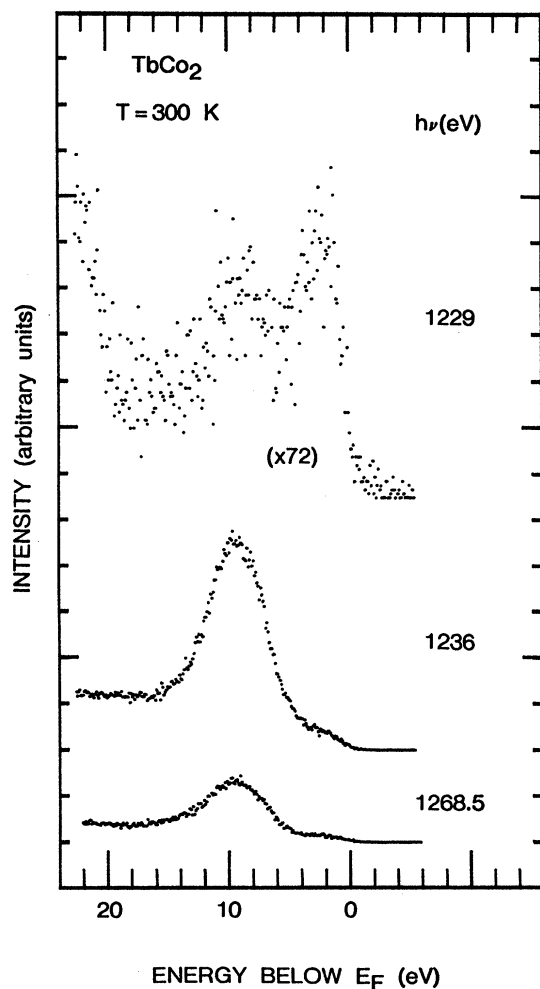


FIG. 3. Valence-band emission of TbCo_2 for several photon energies below and at the Tb $3d$ absorption edges. Curves have vertical zeros, defined by their portions above E_F , displaced upward from the figure boundary by 1, 3, and 8.5 units, but all have same vertical scale, for which one unit is 200 counts/sec, except as labeled.

tensity ratio is not known. Because of the enormous interest in the valence-band emission of cerium compounds,^{11,12} and because it is now clear that $3d$ edge resonance effects can be observed, it is an important future goal to obtain such data with sufficient resolution and signal-to-noise ratio to be spectroscopically useful.

A numerical comparison of the $3d$ and $4d$ resonances at particular photon energies can be made for TbCo_2 as follows. The $4f$ photoemission cross section for photon energies $h\nu_n$ near the nd edge $\sigma(h\nu_n)$ is the sum of normal [$\sigma^0(h\nu_n)$] and resonance [$\sigma^{\text{res}}(h\nu_n)$] parts, and we define the resonance contrast $\xi(h\nu_n) = \sigma(h\nu_n)/\sigma^0(h\nu_n)$. It follows that the ratio α of the $4d$ to $3d$ resonance parts at two particular photon energies is

$$\left[\frac{\sigma^0(h\nu_4)}{\sigma^0(h\nu_3)} \right] \left[\frac{\xi(h\nu_4) - 1}{\xi(h\nu_3) - 1} \right].$$

We now estimate α at the photon energies of maximal reso-

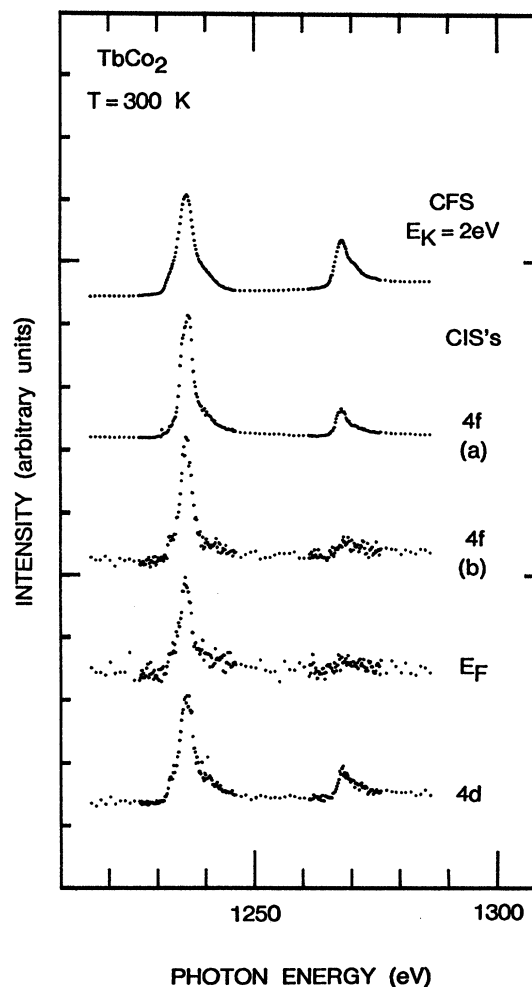


FIG. 4. CFS and CIS spectra for TbCo_2 for photon energies in the $3d$ absorption region. The initial states of the CIS spectra (a) and (b) are the same as in Fig. 2, and E_F denotes the Fermi level.

nance, $h\nu_4 = 156$ eV and $h\nu_3 = 1236$ eV, for the valence-band $4f$ emission 10 eV below E_F . From calculated¹³ values of Ce $4f$ cross sections we estimate $\sigma^0(156 \text{ eV})/\sigma^0(1236 \text{ eV}) \approx \sigma^0(160 \text{ eV})/\sigma^0(1253.6 \text{ eV}) = 906$. Taking $\sigma^0(1236 \text{ eV}) \approx \sigma^0(1229 \text{ eV})$ we have $\xi(1236 \text{ eV}) = 72$ obtained, as stated above, from the data of Fig. 3 and for $\xi(156 \text{ eV})$ we use the calculated¹³ Ce $4f$ cross sections to correct the value of 5, obtained, as stated above, from the data of Fig. 1, by the factor $\sigma^0(120 \text{ eV})/\sigma^0(156 \text{ eV}) \approx \sigma^0(120 \text{ eV})/\sigma^0(160 \text{ eV}) = 1.47$ to give $\xi(156 \text{ eV}) = 7.4$. From these numbers we then find that $\alpha = 82$. Thus $\sigma^{\text{res}}(156 \text{ eV}) > \sigma^{\text{res}}(1236 \text{ eV})$ and the reason that the $3d$ contrast exceeds the $4d$ contrast is that the $3d$ background part is so much weaker. Presumably, the $4d$ resonance is larger than for $3d$ because the $4d$ and $4f$ wave functions are in the same atomic shell.

There are three important potential advantages to using the $3d$ resonance in addition to the $4d$ resonance as a spectroscopic technique. The first is the very large contrast ξ_{3d} obtained. The second is that the increased photon energy yields photoelectrons from the valence band with kinetic en-

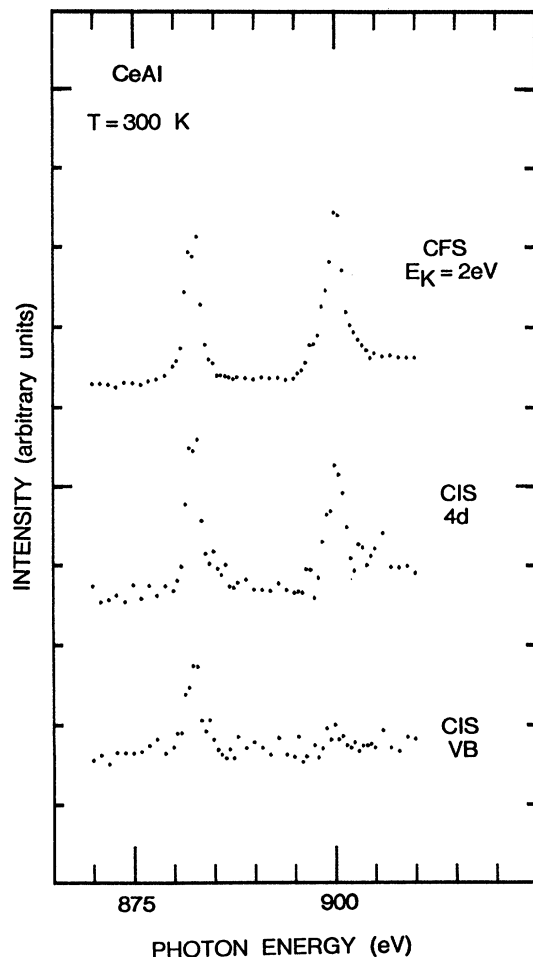


FIG. 5. CFS and CIS spectra for CeAl for photon energies in the $3d$ absorption region. VB denotes the entire unresolved valence-band region. The peaks at ~ 883 eV have 3 counts/sec above a base line of 0 counts/sec, and 10 counts/sec above a base line of 3 counts/sec, respectively, for the VB and $4d$ curves.

ergies considerably higher than that of the elastic escape depth minimum,¹⁴ so that the extent of surface effects in the spectra taken using the $4d$ resonance can be gauged. This has been a pressing issue in the case of studies of cerium $4f$ emission.¹¹ The third arises from the much smaller spectral spreading due to multiplets in the $3d$ spectrum. As noted above the two spin-orbit components of the $3d$ spectrum appear to differ in their resonance efficiency and when this effect is understood it may be useful for sorting differing angular momentum components of the valence-band emission, of great interest in the case of $4f$ and $5d$ emission in cerium materials.¹² Even more exciting is the fact that the absorption peaks associated with different $4f$ valences have been shown¹⁵ to be well separated in $3d$ spectra, which should enable separating $4f$ emission from different valences much more easily than when using the $4d$ absorption edges, where multiplet spreading is often larger than the separation of different valence components.² Again, this is of great importance for the case of cerium,¹² where it is not known if the valence-band emission all arises from a single-valence state, and in mixed-valent rare-earth materials generally.

In summary, we have reported the first observation of resonant enhancement of rare-earth $4f$ photoemission for photon energies near the rare-earth $3d$ edge and have pointed out exciting possibilities for employing this phenomena as a spectroscopic technique if sufficient photon flux in the relevant photon-energy range can be obtained.

It is a pleasure to acknowledge J. M. Lawrence for providing our CeAl sample, W. Ellis and L. Cox for their participation and assistance in the experiment, and P. Pianetta and M. Rowan of the SSRL staff for their able and enthusiastic support. The Stanford Synchrotron Radiation Laboratory is supported by the Office of Basic Energy Sciences of the U.S. Department of Energy and the Division of Materials Research of National Science Foundation (NSF) and part of this work is supported by the NSF under Grant No. DMR-79-13102.

¹W. Lenth, F. Lutz, M. J. Barth, G. Kalkoffen, and C. Kunz, *Phys. Rev. Lett.* **41**, 1185 (1978).

²J. W. Allen, L. I. Johansson, R. S. Bauer, I. Lindau, and S. B. Hagström, *Phys. Rev. Lett.* **41**, 1499 (1978).

³L. I. Johansson, J. W. Allen, T. Gustafsson, I. Lindau, and S. B. Hagström, *Solid State Commun.* **28**, 53 (1978).

⁴J. M. Esteva, R. C. Karnatak, and J. P. Connerade, *J. Electron Spectrosc. Relat. Phenom.* **31**, 1 (1983).

⁵M. B. Chamberlain, A. F. Burr, and R. J. Liefeld, *Phys. Rev. A* **9**, 663 (1974).

⁶E. J. McGuire, *J. Phys. Chem. Solids* **33**, 577 (1972); E. J. McGuire, *Phys. Rev. A* **5**, 1052 (1972).

⁷F. C. Brown, R. Z. Bachrach, and N. Lien, *Nucl. Instrum. Methods* **152**, 73 (1978).

⁸Z. Hussain, I. Umbach, D. A. Shirley, J. Stöhr, and J. Feldhaus,

Lawrence Berkeley Laboratory Report No. LBL-12729 (unpublished).

⁹J. K. Lang, Y. Baer, and P. A. Cox, *J. Phys. F* **11**, 121 (1981).

¹⁰J. M. Lawrence, J. W. Allen, S.-J. Oh, and I. Lindau, *Phys. Rev. B* **26**, 2362 (1982).

¹¹J. W. Allen, S.-J. Oh, I. Lindau, J. M. Lawrence, L. I. Johansson, and S. B. Hagström, *Phys. Rev. Lett.* **46**, 1100 (1981).

¹²J. W. Allen, *J. Less-Common Met.* **93**, 183 (1983).

¹³S. M. Goldberg, C. S. Fadley, and S. Kono, *J. Electron Spectrosc. Relat. Phenom.* **21**, 285 (1981).

¹⁴I. Lindau, W. E. Spicer, *J. Electron Spectrosc. Relat. Phenom.* **3**, 409 (1974).

¹⁵J. C. Fuggle, F. U. Hillebrecht, J.-M. Esteva, R. C. Karnatak, O. Gunnarsson, and K. Schönhammer, *Phys. Rev. B* **27**, 4637 (1983).